Composite Structures 125 (2015) 509–519

Contents lists available at ScienceDirect

Composite Structures

journal homepage: www.elsevier.com/locate/compstruct

Experimental investigation of the mechanical properties of dry microbraids and microbraid reinforced polymer composites

Stefano Del Rosso [a,*], Lorenzo Iannucci [a], Paul T. Curtis [a,b]

[a] Imperial College London, Exhibition Road, SW7 2AZ London, UK
[b] Defence Science and Technology Laboratory, Porton Down, Salisbury SP4 0JQ, UK

ARTICLE INFO

Article history:
Available online 21 February 2015

Keywords:
Microbraids
Robotised filament winding
Polymer-matrix composites

ABSTRACT

This paper presents a comprehensive series of mechanical tests performed on two high performance polymeric fibres, microbraids and microbraid reinforced polymer composites (mBRPC). Quasi-static tests were performed on the raw materials and the effect of different gauge lengths and strain rates investigated. Then, microbraids having sub-millimetre diameters were manufactured from the raw yarns using a Maypole-type braiding machine. The effects of different braid architectures, number of braided yarns and bias angles were assessed through a series of tensile tests on dry microbraids. A novel and unique manufacturing method of aligning microbraids in a unidirectional fashion via robotised filament winding was developed to manufacture microbraid reinforced polymer composites (mBRPC). Quasi-static tensile tests performed on mBRPC showed improved mechanical properties, for certain architectures, with respect to those noted for unidirectional composites manufactured using same technique.

1. Introduction

High performance polymeric fibres are extensively used to make personal protective textiles and as reinforcing phase in polymer composite materials. Thanks to their high tenacity and toughness, low elongation at break as well as the ability to dissipate shock waves over large areas in a short amount of time, they are very suitable for applications where impact resistance and energy absorption capabilities are of vital importance.

Braiding is the process of interlacing three or more threads in such a way that they cross one other and are laid together at a bias angle. In theory, any material, in the form of strips or filaments, can be braided to produce linear, flat, tubular or solid forms. Braids can be produced as 2D, in flat or tubular form, and as 3D structures. The former contains only two sets of strands through the thickness, and axial yarns in case of triaxial braids, whereas the latter have several strands through the thickness. Over the past decades, braided reinforced polymer composites (BRPC) have been increasingly used in high performance structures due to their outstanding properties such as damage and impact resistance, high delamination resistance, greater through-the-thickness reinforcement and lesser notch sensitivity with respect to unidirectional (UD) and woven reinforced composites. Moreover, the investment and labour costs can be minimised due to the inexpensive machinery, high production rate and level of automation which the braiding technique offers [1–3].

Brunnschweiler [4,5] and subsequently Ko and Pastore [1] discussed in details the principles of braid manufacture and the use of braided fabrics as reinforcing phase within engineering structures. Recently, Carey and Ayranci [6] reviewed the published studies on 2D braided composites outlining advantages and disadvantages of this technique, different characterisation methods currently employed and applications of BRPC in the composite industry. Omeroglu [7] investigated the properties of dry 2D polypropylene (PP) braided ropes by varying the braid architecture, fibre linear density and take-up speed. Regular braids showed higher tenacity, modulus and yield strength with respect to diamond braids. The higher the take-up speed, the higher the aforementioned properties. Moreover, the Young's modulus and tenacity were noted to be higher for braids made of finer PP strands. Harte and Fleck [8] studied the tensile behaviour of glass–epoxy braided tubes having different braid angles. Although they noted a lower Young's modulus and tensile strength with increasing fibre bias angle, the strain to failure and the energy absorption increased for the same angles. Moreover, the failure mechanism of the tubular composites changed from brittle to ductile with increasing the fibre bias angle from 23° to 55°.

Usually, braided reinforced composites are produced by stacking many braided slit sleeves or flattened tubes in order to create

* Corresponding author.
E-mail address: stefano.delrosso@imperial.ac.uk (S. Del Rosso).

http://dx.doi.org/10.1016/j.compstruct.2015.02.036
0263-8223/

Table 1
Physical properties of the investigated materials.

Yarns	Density (g/cm^3)	Linear density (dtex)	Single fibre diameter (μm)	No. filaments/yarn
Dyneema®SK75	0.97	220	17.28 ± 0.58 (112)	100
Kevlar®49	1.44	215	12.14 ± 0.41 (108)	130
Matrix	Density (g/cm^3)	Areal density (g/m^2)	Thickness (μm)	
Rayofix TP	0.932	71.63	75	

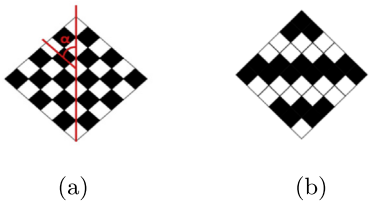

Fig. 1. Braid patterns: (a) Diamond 1/1; (b) Regular 2/2.

layers of desired orientation and thickness. For instance, Kelkar et al. [9] investigated the tensile and fatigue properties of epoxy-reinforced laminates made from 2/2 carbon braid slit sleeves and flattened braided tubes. As the fibre bias angle increased, the ultimate tensile strength and Young's modulus of the composites decreased whilst the endurance increased with respect to increasing braid angle. Fouinneteau and Pickett [10] studied the properties of carbon and glass braided composites made from flattened braided tubes and thermoset epoxy resin. For the same braid angle, they noted a higher tensile strength and strain to failure for the carbon braided composites. However, premature failure occurred locally in the region close to the specimen tabbed area, regardless of the material. The tensile strength and strain to failure of the carbon braided composites were detrimentally affected by as much as 27.5% and 39.1%, respectively, when the specimens had cut edges. Falzon and Herszberg [11] found a reduction of 20% in the tensile strength of braided composite laminates with respect to UD ones. They attributed this reduction to fibre damage while braiding.

To the authors' best knowledge, there are very few studies in the open literature in which the mechanical behaviour of braids and microbraids made of high performance polymeric fibres has been experimentally assessed (for example, in [7,12–14]). Moreover, there are no existing studies of microbraids directly used as reinforcing phase in composite materials. Sakaguchi et al. [15] and Fujihara et al. [16] claim the manufacture of microbraid reinforced composites. They braided matrix filaments over high performance fibres. The manufactured braids were filament wound over a steel plate and then cured. However, after melting the braided filaments, a composite material reinforced by unidirectional fibres would appear. Moreover, a linear density of the used microbraids above 10,000 dtex (the microbraid's diameter and linear density was not stated in either paper) would not be truly applicable to a "micro" range of dimensions.

The main aim of this work is to investigate the potential use of 2D microbraids as the primary constituent in high performance textiles and as the reinforcing phase within polymer composite systems. In this contest, the present investigation is concerned with the mechanical characterisation of high performance polymeric yarns and 2D microbraids. A comprehensive series of

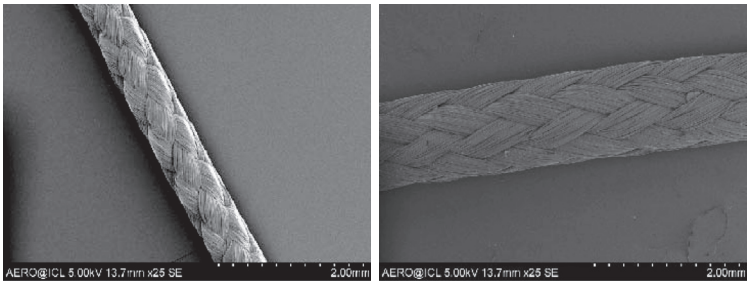

Fig. 2. SEM images of two different microbraids: (a) bDA1, (b) bKA2.

Table 2
Physical properties of the manufactured microbraids.

bID	Material	Number of braided yarns	Braid pattern	Braid diameter (mm)	Braid angle (°)	Linear density (dtex)
bDA1	Dyneema®SK75	8	1/1	0.86 ± 0.02	15.0 ± 0.8	1816 ± 54
bDB1	Dyneema®SK75	8	1/1	0.85 ± 0.02	19.3 ± 1.3	1996 ± 48
bDC1	Dyneema®SK75	8	1/1	0.67 ± 0.01	28.7 ± 1.1	2238 ± 61
bDA2	Dyneema®SK75	16	2/2	1.34 ± 0.01	22.0 ± 0.6	3878 ± 59
bDB2	Dyneema®SK75	16	2/2	1.2 ± 0.01	31.9 ± 1.5	4419 ± 66
bDC2	Dyneema®SK75	16	2/2	0.97 ± 0.01	43.9 ± 0.7	5066 ± 48
bKA1	Kevlar®49	8	1/1	0.84 ± 0.02	13.1 ± 0.7	1890 ± 57
bKB1	Kevlar®49	8	1/1	0.84 ± 0.01	23.9 ± 0.5	1934 ± 64
bKC1	Kevlar®49	8	1/1	0.69 ± 0.02	39.1 ± 0.9	2026 ± 53
bKA2	Kevlar®49	16	2/2	1.25 ± 0.01	21.7 ± 1.6	3920 ± 62
bKB2	Kevlar®49	16	2/2	1.12 ± 0.01	28.6 ± 1.4	4117 ± 49
bKC2	Kevlar®49	16	2/2	0.98 ± 0.01	40.1 ± 1.1	4478 ± 69

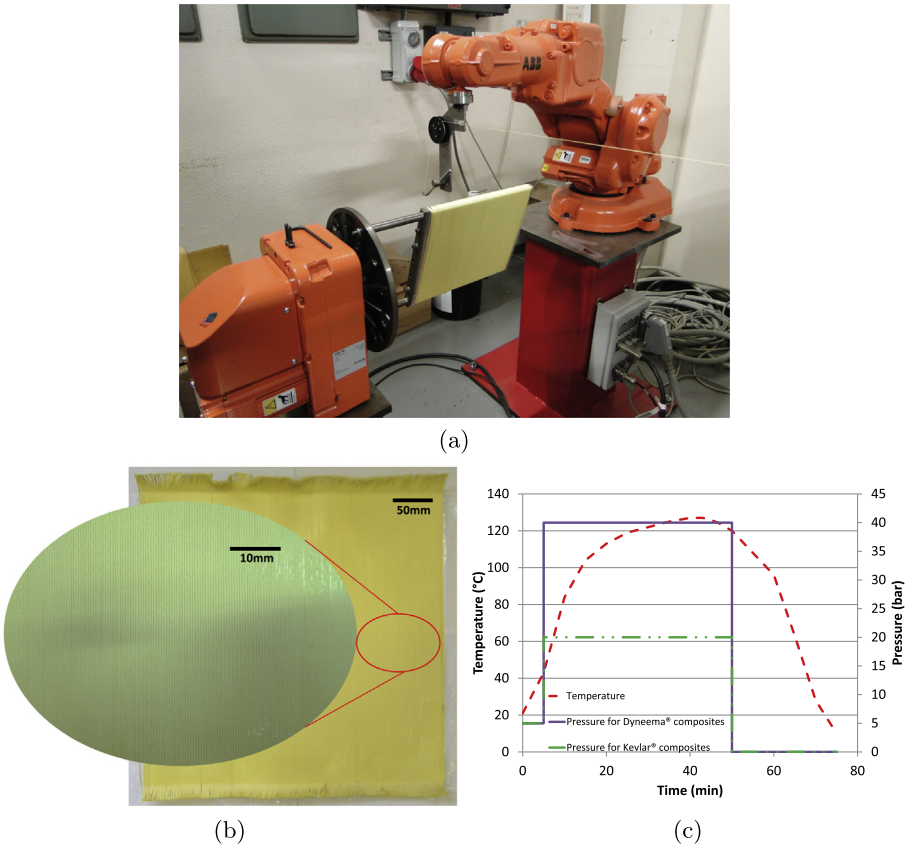

Fig. 3. mBRPC manufacture: (a) Robotised filament winding; (b) cKA1 prepreg; (c) Temperature vs. Pressure consolidation profile.

Table 3
Physical properties of the manufactured composites.

cID	Number of layers	Stacking sequence	Laminate thickness (mm)	Areal density (kg/m^2)	Fibre volume fraction (%)	Void content (%)
cDUD	10	$[0/(90_2/0_2)_2/90]$	3.99 ± 0.24	2.81 ± 0.02	72.50 ± 1.18	6.54 ± 1.06
cDA1	10	$[0/(90_2/0_2)_2/90]$	3.56 ± 0.16	2.70 ± 0.03	68.24 ± 1.32	7.55 ± 1.27
cDB1	10	$[0/(90_2/0_2)_2/90]$	3.79 ± 0.19	2.83 ± 0.05	78.66 ± 0.83	7.72 ± 0.61
cDC1	10	$[0/(90_2/0_2)_2/90]$	4.51 ± 0.23	3.51 ± 0.03	81.06 ± 1.40	7.66 ± 1.28
cDA2	6	$[0/90]_3$	3.06 ± 0.23	2.21 ± 0.02	73.94 ± 1.82	8.73 ± 1.64
cDB2	6	$[0/90]_3$	3.28 ± 0.18	2.45 ± 0.02	77.46 ± 0.70	7.13 ± 0.59
cDC2	6	$[0/90]_3$	3.76 ± 0.22	2.88 ± 0.02	80.52 ± 2.21	6.03 ± 2.09
cKUD	10	$[0/(90_2/0_2)_2/90]$	3.11 ± 0.15	2.78 ± 0.03	61.08 ± 1.39	10.48 ± 1.15
cKA1	10	$[0/(90_2/0_2)_2/90]$	3.10 ± 0.25	2.80 ± 0.11	67.85 ± 2.18	12.97 ± 1.54
cKB1	10	$[0/(90_2/0_2)_2/90]$	3.45 ± 0.16	2.83 ± 0.01	67.32 ± 0.63	13.68 ± 0.59
cKC1	10	$[0/(90_2/0_2)_2/90]$	4.48 ± 0.22	3.79 ± 0.18	64.43 ± 2.70	16.61 ± 1.95
cKA2	6	$[0/90]_3$	2.64 ± 0.28	2.21 ± 0.01	63.43 ± 0.65	13.46 ± 0.54
cKB2	6	$[0/90]_3$	2.66 ± 0.12	2.44 ± 0.02	61.7 ± 1.13	16.90 ± 0.94
cKC2	6	$[0/90]_3$	3.99 ± 0.23	3.02 ± 0.09	53.87 ± 1.24	28.11 ± 0.77

mechanical tests is presented and results reported. Thus, a novel and unique method was developed and used to manufacture microbraid reinforced polymer composites (mBRPC) via robotised filament winding and hot-pressing. The manufactured mBRPC were tested in tension and results herein presented.

2. Materials, manufacture and testing methods

2.1. Materials

Two high performance yarns were investigated in this study: Dyneema®SK75 and Kevlar®49. Fibre diameters were determined by analysis of images from scanning electron microscope (SEM). For the manufacture of microbraid reinforced composites, Rayofix TP, a thermoplastic resin film, was used. Physical properties of the investigated materials are listed in Table 1. The number in brackets indicates the number of single fibres examined.

2.2. Manufacture of dry microbraids

The manufacture of 2D microbraids was carried out using the Herzog RU2-16/80, a Maypole-type braiding machine having two working heads, 8 horn gears per head and equipped with 16 carriers in the "fully-occupied" setup. In order to determine the influence of the braiding architecture and the number of braided yarns on the mechanical properties of the microbraids, diamond 1/1 and regular 2/2 patterns were created by varying the number of working carriers and the carrier disposition on the braiding path, respectively. The different braid patterns are sketched in Fig. 1. For each braid architecture, microbraids having different braid angle α

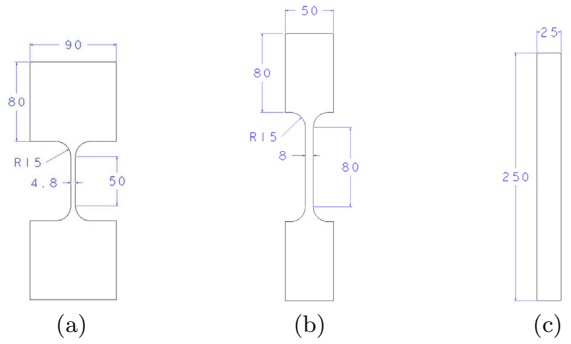

Fig. 4. Geometries of the tensile specimens for: (a) Unidirectional composites; (b) Dyneema®SK75 mBRPC; (c) Kevlar®49 mBRPC. All dimensions in mm.

were manufactured by changing the cogwheel ratio on the braiding machine. The diameter of the microbraids and their bias angles were determined by analysis of SEM images (Fig. 2). The microbraids linear densities were determined according to the ASTM D1577-07 Standard Test Methods for Linear Density of Textile Fibers [17]. Specifications of the manufactured microbraids are presented in Table 2.

A generic dry microbraid will belong to the class "bXYZ", where:

- b stands for dry microbraid.
- X will be the microbraid's material, in particular D for Dyneema®SK75 and K for Kevlar®49.
- Y will denote the braid angle, where A < B < C.
- Z will represent the braiding architecture, in particular "1" for diamond 1/1 and "2" for regular 2/2.

2.3. Manufacture of microbraid reinforced polymer composites (mBRPC)

The manufactured microbraids were wound in a unidirectional fashion over a spinning aluminium plate using a robotised filament winding system (Fig. 3(a)). The robot was programmed to move across the plate a distance equal to the diameter of the microbraid per each revolution of the plate. The tension of the rewinding process was controlled by a motor-driven creeling machine able keep the tension constant by changing the material supplying rate. After the winding process was completed, the plate was removed from the motor flange, the thermoplastic film was wrapped over the faces of the dry fabric and finally placed in the hot-press for the consolidation stage. When the plate was cold, the resin-impregnated fabric

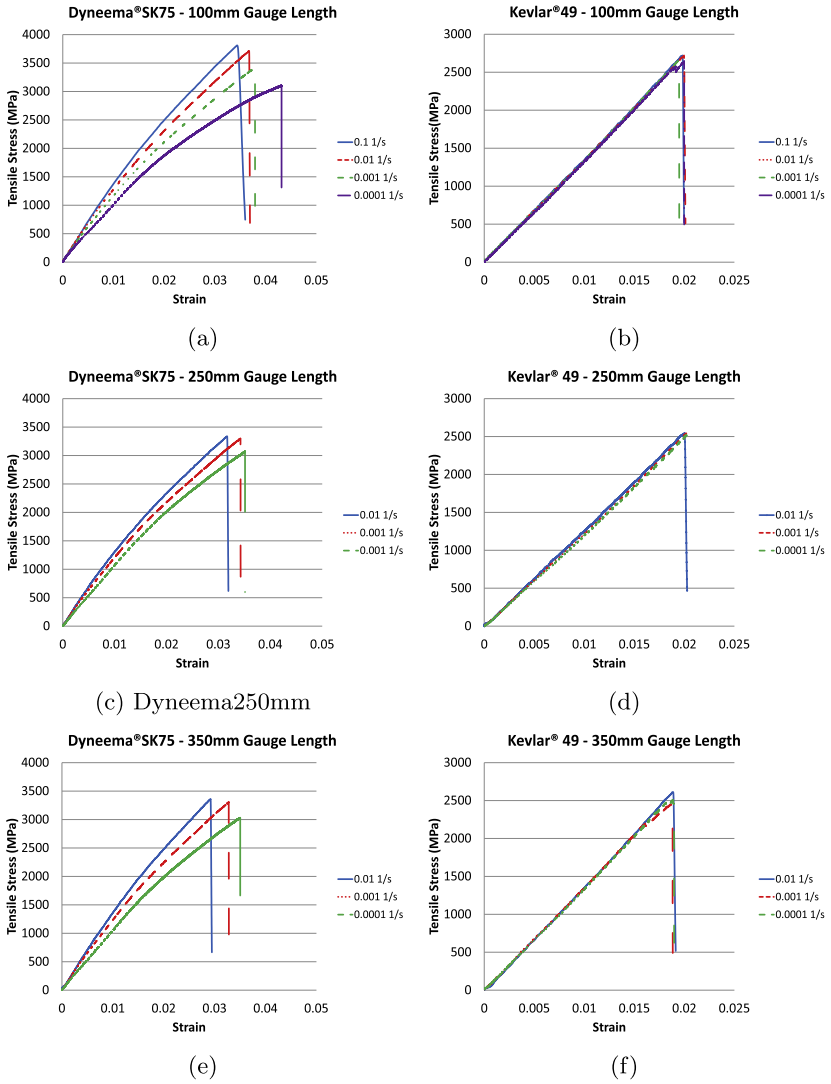

Fig. 5. Engineering stress vs. strain curves for different fibre gauge lengths: (a), (c) and (e): Dyneema®SK75; (b), (d) and (f): Kevlar®49.

was cut from the edges of the plate to obtain two prepregs (Fig. 3(b)). Hence, the latter were hand laid-up in a cross-ply orientation to create the final composite panels. The temperature profile used for curing the microbraid fabrics was identical for both materials. However, the pressure used to consolidate the Kevlar®49 microbraid fabrics was lower than the one used for consolidating the Dyneema®SK75 ones. The temperature vs. pressure profile is shown in Fig. 3(c). In order to directly compare the properties of the mBRPC with cross-ply laminates made with unidirectional fibres and manufactured via the same route, composites having similar areal density and fibre volume fraction were manufactured from Dyneema ®SK76 1760dtex and Kevlar®49 1580dtex, respectively. The mBRPC fibre volume fraction was determined according to the ASTM D3171–11 Standard Test Methods for Constituent Content of Composite Materials [18], whereas the void content was determined according to ASTM D2734-09 Standard Test Methods for Void Content of Reinforced Plastics [19]. Physical properties of the manufactured composites are listed in Table 3. The different lamination sequence for the UD-fibre composites and mBRPC reinforced with 8 yarn microbraids rose not only to keep the fibre volume fraction as high as possible and fairly constant among different composites, but also to maintain the same cross-ply stacking sequence. The generic microbraid reinforced composite "cXYZ" was manufacture using the microbraid "bXYZ".

2.4. Testing methods

Quasi-static tensile tests on yarns were performed at room temperature using an Instron 5969 universal tensile testing machine equipped with a 50kN load cell having an accuracy of ±0.5% of the displayed force. Specimens were clamped using Instron 2714-004 pneumatic capstan grips. Up to 2500 data-points per second were recorded by the acquisition system during each test. The strain was measured by a high speed camera: two points were marked along the gauge length and their relative displacement subsequently measured by motion tracking software developed in house. In order to investigate the effects of the strain rate and gauge length on the aforementioned yarns, tensile tests were performed with three different gauge lengths of 100 mm, 250 mm and 350 mm, and at three different strain rates of 0.01 s^{-1}, 0.001 s^{-1} and 0.0001 s^{-1}, respectively. Only for a gauge length of 100 mm, tensile tests were performed at a strain rate of 0.1 s^{-1}. For each test series, at least 5 valid tests (failure within the gauge length) were performed and collected.

Yarns were also cyclic loaded up to different force levels. This was done to understand to what extent a pre-stress introduced in the yarns prior to be braided would influence the final mechanical properties of the dry microbraids, and also any possible deformation due to stress relaxation of the created architecture. The test

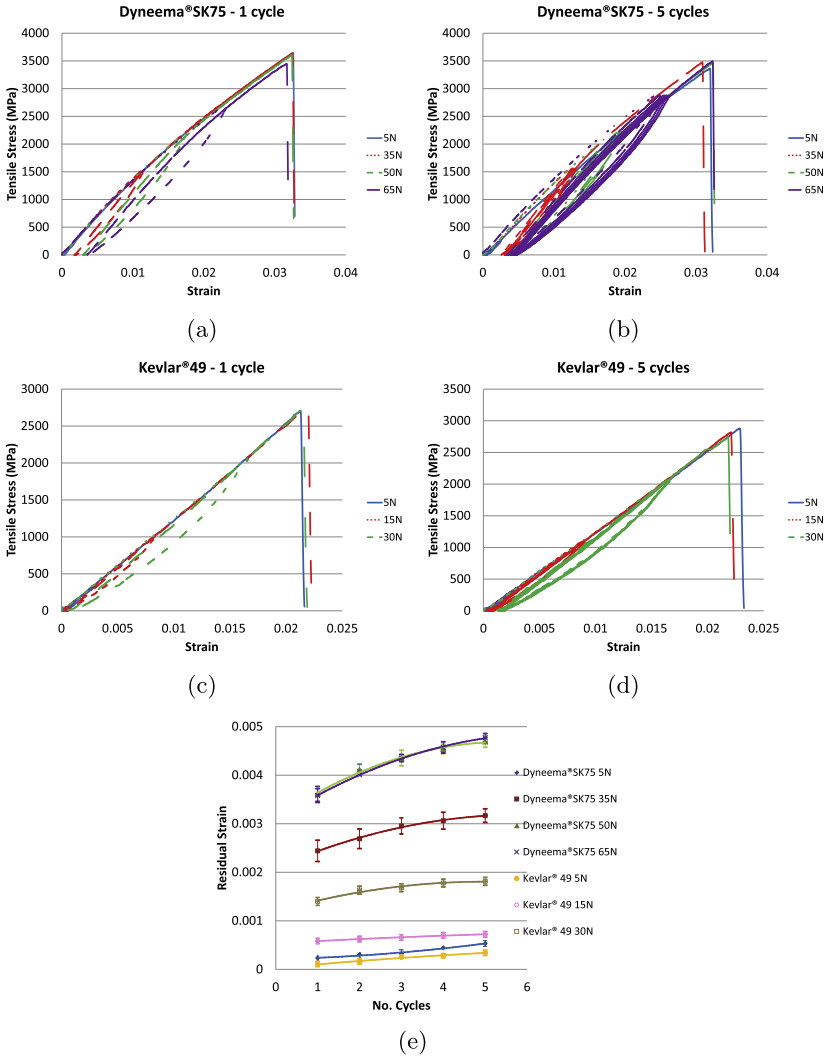

Fig. 6. Cyclic tensile stress vs. strain curves for: (a) Dyneema®SK75 1 cycle; (b) Dyneema®SK75 5 cycles; (c) Kevlar®49 1 cycle; (d) Kevlar®49 5 cycles; (e) Residual strain vs. Number of cycles.

rate was kept constant throughout the loading and unloading parts at 0.01 s^{-1}. One and five consecutive loading and unloading cycles were performed on both fibres, respectively. Same equipment and data acquisition settings used for the tensile tests were adopted for cyclic tests.

Tensile tests on dry microbraids were performed at only one gauge length and strain rate (250 mm and 0.01 s^{-1}, respectively), using the same tensile testing machine and procedures adopted for testing the raw yarns.

Quasi-static tensile tests on mBRPC were performed at room temperature using an Instron 5985 universal testing machine equipped with a 250 kN load cell having an accuracy of ±0.5% of the displayed force. Testing specimens, waterjet cut from the manufactured plates, were clamped using hydraulic grips to prevent slippage. Up to 50 data-points per second were recorded by the acquisition system. Strain was measured contactlessly by a camera tracking the relative displacement of points drawn along the gauge length of the specimens. All tests have been performed at cross-head speed of 10 mm/min. Specimen geometries are sketched in Fig. 4 (all dimensions are in mm).

3. Results

3.1. Quasi-static tensile test

Fig. 5 shows the engineering stress vs. strain curves for Dyneema®SK75 and Kevlar®49 yarns. Only one curve among the tests performed is shown for clarity purposes. It can be seen that Kevlar®49 yarn had a reasonable linear response up to failure regardless of the strain rate at which the yarn was tested. The Young's modulus, tensile strength and strain were little affected by changing the test speed for a fixed gauge length, meaning a very small dependency of the aforementioned mechanical properties over the investigated gauge lengths. A small decrease in tensile strength and strain to failure was noted with increasing gauge length and strain rate by as much as 9% and 4%, respectively. The consistency of the test results would imply an even distribution of defects and flaws along the length of the yarn although the likelihood of finding weaker points would be higher in longer fibres.

On the other hand, the tensile behaviour of Dyneema®SK75 yarn showed a marked dependence with respect to the testing conditions. The Young's modulus increased with increasing strain rate by as much as 17% and 23% over the investigated gauge lengths and strain rates, respectively. The tensile strength remained reasonably constant, within the scatter errors, over the investigated gauge lengths, meaning an even distribution of flaws and defects along the length of the yarn. However, it increased as much as 23% over the investigated strain rates. This is clearly due to the viscoelastic nature of the material itself.

Despite the energy absorption of the two investigated yarns were very similar for the same testing conditions, the toughness and tenacity calculated for Dyneema®SK75 were superior to those noted for Kevlar®49. This is because of the higher strength and strain to failure, as well as lower specific density of the former material with respect to the latter.

3.2. Cyclic tensile tests

Fig. 6 presents the stress vs. strain curves from cycling tests up to different force levels performed on Dyneema®SK75 and Kevlar®49 yarns, respectively. Only one curve among the performed tests is shown for clarity purposes.

It is evident from Fig. 6(a) and (b) that, after the first cycle, a residual strain remained in the Dyneema®SK75 yarn. When the yarn was stressed during the loading part of the test, the polymeric chains were further aligned to the loading direction and the deformation occurring during this stretching was not fully recovered within the unloading time. The residual strain was dependent on the level of load at which the fibre was pre-stressed prior to being brought to failure. The higher the pre-stress, the bigger the residual strain in the fibre. It was also evident an increase in the slope of the second loading part of the stress vs. strain curve with respect to the monotonic one. This is probably due to the better alignment of the polyethylene chains to the loading direction after being straight-

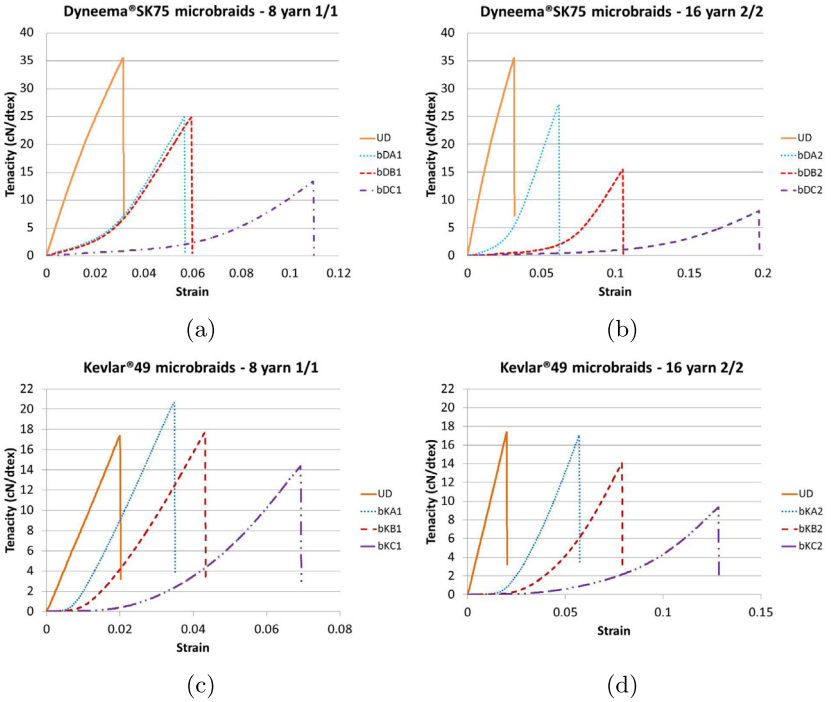

Fig. 7. Tenacity vs. strain curves for different microbraids: (a) Dyneema®SK75 8y 1/1; (b) Dyneema®SK75 16y 2/2; (c) Kevlar®49 8y 1/1; Kevlar®49 16y 2/2.

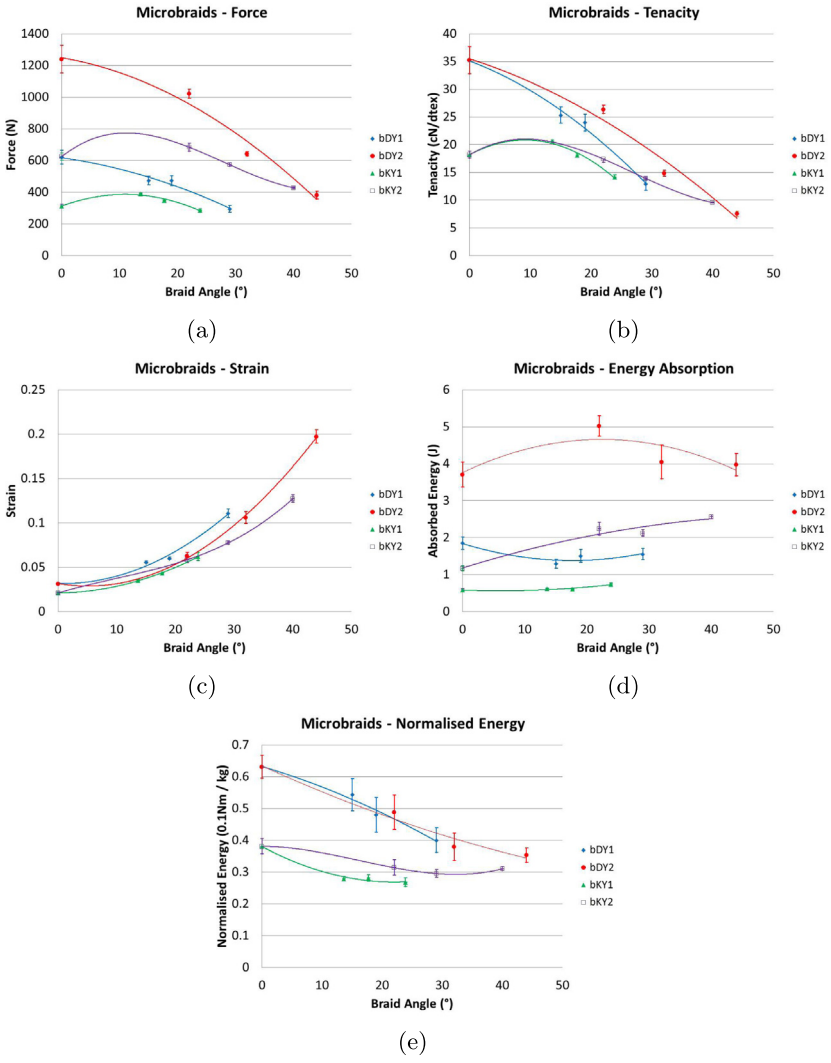

Fig. 8. Tensile properties of dry microbraids: (a) Force vs. braid angle; (b) Tenacity vs. braid angle; (c) Strain vs. braid angle; (d) Energy absorption vs. braid angle; (e) Normalised energy absorption vs. braid angle.

ened out, as also reported by Berger et al. [20]. Once completing the first cycle, the tensile strength and strain to failure of Dyneema®SK75 were noted to be the same, within the scatter error, as if the yarn was not cyclic loaded, i.e. the fibre were not damaged during the cycle. As the number of loading and unloading cycles increased, the residual strain did so although it tended to level off for higher number of cycles (Fig. 6(e)).

On the other hand, the cyclic loading history had very little influence on the mechanical response of Kevlar®49, which residual strain did not exceed 0.17% when the fibre was pre-loaded at ~75% of the maximum yarn breaking force. As seen for Dyneema®SK75 yarns, the tensile strength and strain of Kevlar®49 was not affected by the number of cycling loadings.

Van der Werff and Pennings [21] described the possible mechanisms occurring in ultra high molecular weight polyethylene (UHMwPE) fibres during tensile and cyclic loads. The proposed flow mechanism assumed an induced flow of the polymeric chains due to thermal activated processes - in this case the cyclic tensile deformation. This effect would be much greater in materials having a low melting temperature (T_m) such as UHMwPE than in para-aramids, which T_m is about three time higher. It should be also noted the differences in the chemical structure between the two materials. While UHMwPE has the simplest monomer and chemical structure among all polymers, its chains

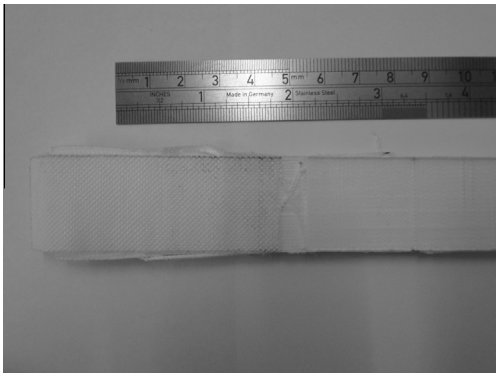

Fig. 9. Dyneema®SK75 mBRPC rectangular specimen incorrectly failed at the gripped region.

are easily prone to deform under external loads, i.e. the C–H bonds and $C\widehat{H}C$ angles along the carbon backbones can be easily stretched, rotated and opened, while the stiffer, benzene ring-rich structure and stronger intramolecular forces present in the aramid fibre make this polymer less prone to deform and faster in recovering the original, more stable, entropy favourable conformation.

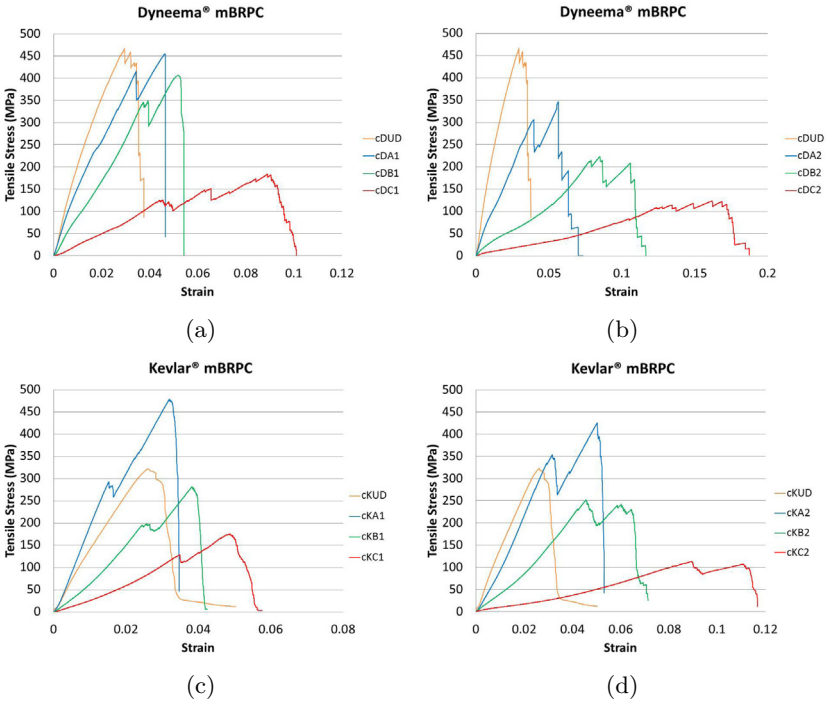

Fig. 10. Engineering stress vs. strain curves for different microbraid reinforced composites: (a) cDY1; (b) cDY2; (c) cKY1; cKY2.

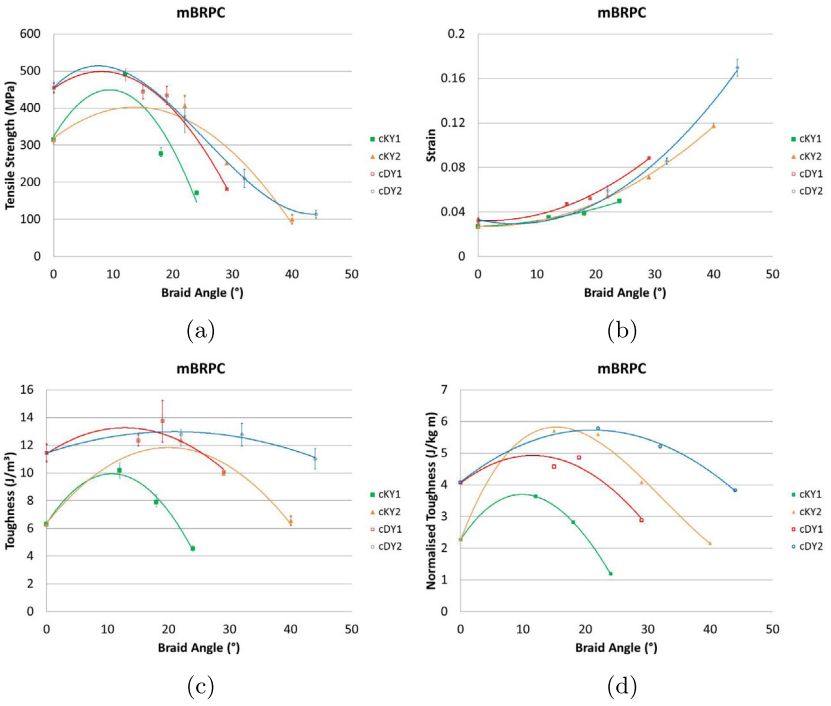

Fig. 11. Tensile properties of microbraid reinforced polymer composites: (a) Tensile strength vs. braid angle; (b) Strain vs. braid angle; (c) Toughness vs. braid angle; (d) Normalised energy absorption vs. braid.

3.3. Quasi-static tensile test on dry microbraids

The results obtained from cycling tests of Dyneema®SK75 and Kevlar®49 showed that these yarns experienced a deformation even when stressed at small loads. Although this deformation would be small and possibly time-recoverable [21], the tension in the yarn during the spooling process was controlled to not exceed 2 N tension in order to minimise any possible physical change in the raw materials and in the architecture of the braid after being shaped. On the other hand, the rewinding speed and the carriers revolution speed was kept high at 120 m/min and 300 rpm, respectively, in order to not give to the polymeric chains

enough time to respond to the external load. Higher processing speeds, as well as low working tensions, would minimise the residual strain in the fibre after the external stresses are removed.

Fig. 7 shows the tenacity vs. strain curves for Dyneema®SK75 and Kevlar®49 microbraids obtained from quasi-static tensile tests. Engineering properties are graphically presented in Fig. 8. It clearly appears that the braid angle, defined as the angle between the braid axial direction and the bias yarns, played a fundamental role in determining the final properties of the dry microbraids. The strain to failure approached 20% for sample bDC2, i.e. more than five times higher the strain to failure of the relative UD counterpart. The higher the bias angle, the higher the strain to failure. On the other hand, it can be seen that microbraids having smaller braid angles had a stiffer response after jamming occurred with respect to those having bigger bias angles. It also appears from Fig. 7 that the tenacity of the investigated microbraids tended to diminish with increasing braid angle. Although this was always true for Dyneema®SK75 microbraids, however, the tenacity of bKA1 and bKA2 samples was higher than the tenacity of their unidirectional counterpart by as much as 17.51% and 3.17%, respectively, despite their higher linear densities and crimped yarns. It is reasonable to think that the mechanical interlocks created during the braiding process would prevent an early failure of the whole structure, i.e. the microbraid was still able to withstand the external load even though the structure was damaged and some filaments already failed. The reason why this effect appeared only in Kevlar®49 microbraids would be due to the higher coefficient of friction with respect to that of Dyneema®SK75. The fibre–fibre coefficient of friction for Dyneema®SK75 yarn is reported to be 0.05–0.065 [22,23] whereas the fibre–fibre coefficient of friction for Kevlar®49 yarns is as high as 0.15–0.22 [23,24]. The higher coefficient of friction of Kevlar®49 yarns would make more difficult the sliding of the yarns and the rearrangement of the braid geometry under external load. In fact, the jamming point of Kevlar®49 microbraids would occur at lower strains with respect to Dyneema®SK75 microbraids for the same braid angle and braid diameter. The rubbing of the jammed yarns would give extra strength to the braid structure. However, when normalising the area under the tenacity vs. strain curves with respect to the microbraid linear density, the normalised energy values obtained for Dyneema®SK75 and Kevlar®49 dry microbraids were always lower with respect to those noted for the respective UD counterparts. Although the normalised energy absorption ability of Dyneema®SK75 decreased with increasing linear density, there was no significant difference in normalised energy amongst Kevlar®49 microbraids having the same architecture but different α, meaning that the capacity of absorbing energy of these microbraids is approximately the same regardless of the braid angle and the linear density.

3.4. Quasi-static tensile test on mBRPC

Tensile tests on mBRPC were performed according to ASTM D3039-08 Standard Test Method for Tensile Properties of Polymer Matrix Composite Materials [25]. Preliminary test results on unidirectional composites and Dyneema®SK75 mBRPC performed using rectangular specimens were unsuccessful (Fig. 4(c)). Specimens failed at the gripped region (Fig. 9) due to the low shear strength of the composites. As pointed out in different papers [26,27], it is very difficult to introduce axial stresses from the tabbed regions of the specimen to its gauge length by shear, especially for slippery, low shear strength materials. Therefore, in order to promote failure within the gauge length, specimens having larger dogbones and narrower width of the gauge part were waterjet cut from the manufactured panels (Fig. 4(a) and (b)).

Fig. 10 shows the engineering stress vs. strain behaviour for Dyneema®SK75 and Kevlar®49 microbraid reinforced composites.

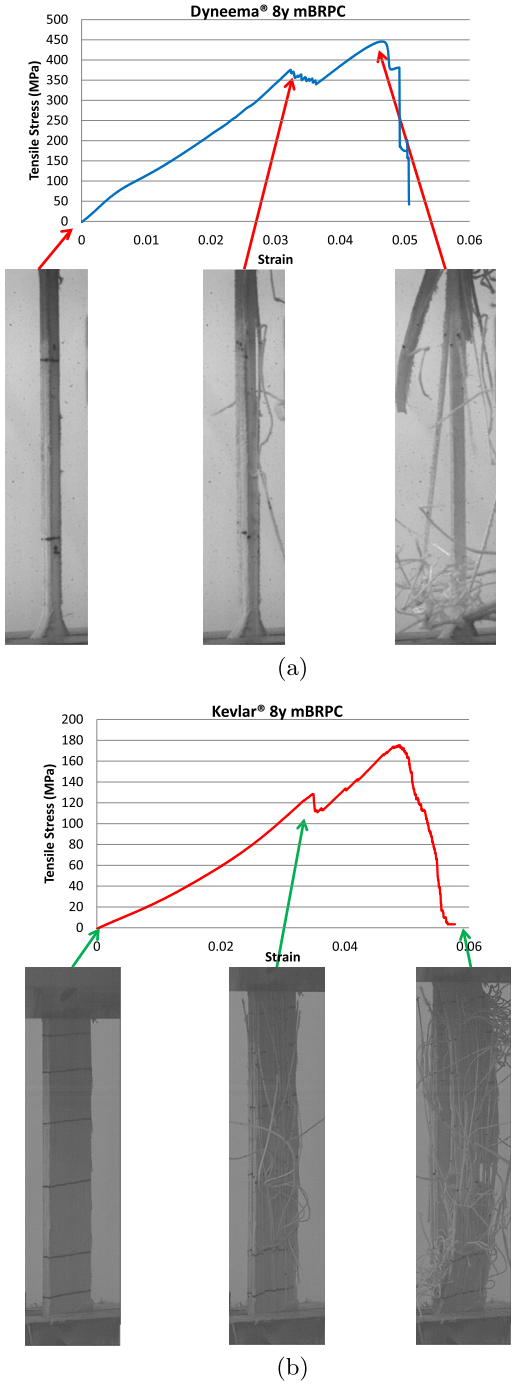

Fig. 12. mBRPC failure: (a) cDA1; (b) cKC1.

Only one curve among the tests performed is shown for clarity purposes. Engineering properties are graphically shown in Fig. 11.

It can be observed from Fig. 10 that the stress vs. strain curves of both Dyneema®SK75 and Kevlar®49 microbraid reinforced composites had similar trends observed when testing dry microbraids. The smaller the braid angle, the higher the tensile strength. On the other hand, the higher the braid angle, the higher the strain to failure. However, the failure mode of mBRPCs was different from the brittle-catastrophic mode of failure experienced by the dry microbraids. In proximity of failure, the outermost layers of the microbraid reinforced composites failed, making the load to drop slightly (Fig. 12). Nevertheless, the specimen was still able to carry the external load until complete failure occurred thereafter.

Delamination occurred prior to failure in all tested specimens. Moreover, the higher the yarns bias angle, the higher the extent of delamination among the laminate layers, which can be also deducted by the smoother fall of the stress vs. strain curves after ultimate tensile strength, for both materials.

The strain to failure of each microbraid reinforced material is comparable, within the scatter errors, with the strain to failure of the constituent microbraid by which the panel was manufactured. For Dyneema®SK75 mBRPC, the tensile strength of the laminates decreased with increasing braid angle and no significant differences can be appreciated between composites reinforced with microbraids made of 8 and 16 yarns, as far as the tensile strength is concerned. The toughness, calculated as the area under the stress vs. strain curve, remained fairly constant regardless of the braid angle at the value of the unidirectional composites manufactured using same technique. However, this property tended to diminish with increasing braid angle. On the other hand, the ultimate tensile strength of Kevlar®49 mBRPC manufactured by braids having the smallest braid angle was higher than the ultimate tensile strength of the unidirectional counterpart by as much as 55.7% and 28.9% for composites reinforced with 8 yarn and 16 yarn microbraids, respectively. Coupling the higher strength with higher strain to failure, the toughness of these two particular composites was higher than the toughness calculated for the unidirectionally aligned fibre composites by as much as 61.3% and 96.2%, respectively. Normalising the toughness with respect to the areal density of the manufactured composites, it appears from Fig. 11(d) that laminates reinforced with microbraids having small braid angle had superior ability to absorb energy with respect to laminates reinforced with unidirectional fibres, for both materials, although this property tended to diminish with increasing braid angle. This result can be attributed to the inherent nature of the braid, which structure made of mechanically intertwined threads could help to distribute more uniformly the external load throughout the whole structure. However, these observations must be confirmed with other experimental tests in order to assess to what extent the difference in specimen geometry, thickness, fibre volume fraction and areal density affected the mechanical response of this novel class of composite materials.

4. Conclusion

In this paper, the tensile response of two high performance fibres were experimentally investigated via a comprehensive series of mechanical tests. Experimental results showed a significant difference in the tensile behaviour of the investigated materials as far as the stress vs. strain behaviour is concerned. Different types of microbraids were manufactured from the as supplied yarns. Both Dyneema®SK75 and Kevlar®49 microbraids showed different tensile properties with respect to those observed for the constitutive materials. The final mechanical properties of braids depended not only on the material properties but also on the fibre bias angle and architecture. As the braid angle increased, also the strain to failure did so although whilst the tenacity decreased. However, for some architectures and braid angles, the tenacity of the dry microbraids exceeded the tenacity of the unidirectional yarn.

In order to manufacture microbraid reinforced polymer composites having high fibre volume fraction, a robotised filament winding system and hot-pressing technique were successfully employed. Tensile tests on specimens waterjet cut from the manufactured composites showed always higher strain to failure when compared with unidirectional composites made using the same manufacturing route. Moreover, for certain braid angles, it was also noted a 55.7% higher tensile strength and a 96.2% higher toughness. The progressive failure mode noted when tensile testing the mBRPCs would imply more damage tolerant structures able to absorb more external energy prior to failure.

The results of this study indicate that the braiding process can be used to manipulate and modify, to some extent, the mechanical properties of the precursor materials for the creation of new materials with unique and enhanced mechanical properties. Further research needs to examine the mechanical properties of dry microbraids and mBRPC under dynamic loading conditions in order to demonstrate the applicability of microbraid reinforced systems in high energy absorption applications.

Acknowledgements

The authors would like to acknowledge the funding from DSTL MAST STC and EPSRC under CASE award DSTL-X-1000061561. DSM Dyneema and DuPont® are acknowledged for the provision Dyneema®SK75 and Kevlar®49 yarns, respectively.

References

[1] Head A, Ko F, Pastore C. Handbook of industrial braiding. Atkins and Pearce; 1989.
[2] Lee S. Handbook of composite reinforcements. Wiley; 1992.
[3] Cox B, Flanagan G. Handbook of analytical methods for textile composites, NASA contractor report, National aeronautics and space administration; 1997.
[4] Brunnschweiler D. Braids and braiding. J Text Inst Proc 1953;44(9):P666–86. http://dx.doi.org/10.1080/19447015308687874.
[5] Brunnschweiler D. The structure and tensile properties of braids. J Text Inst Trans 1954;45(1):T55–77. http://dx.doi.org/10.1080/19447025408662631.
[6] Ayranci C, Carey J. 2d braided composites: a review for stiffness critical applications. Compos Struct 2008;85(1):43–58. http://dx.doi.org/10.1016/j.compstruct.2007.10.004.
[7] Omeroglu S. The effect of braiding parameters on the mechanical properties of braided ropes. Fibres Text East Eur 2006;14(4):53–7.
[8] Harte A-M, Fleck NA. On the mechanics of braided composites in tension. Eur J Mech – A/Solids 2000;19(2):259–75. http://dx.doi.org/10.1016/S0997-7538(99)00164-3.
[9] Tate JS, Kelkar AD, Whitcomb JD. Effect of braid angle on fatigue performance of biaxial braided composites. Int J Fatigue 2006;28(10):1239–47. http://dx.doi.org/10.1016/j.ijfatigue.2006.02.009 [The third international conference on fatigue of composites the third international conference on fatigue of composite].
[10] Fouinneteau M, Pickett A. Shear mechanism modelling of heavy tow braided composites using a meso-mechanical damage model. Compos Part A: Appl Sci Manuf 2007;38(11):2294–306. http://dx.doi.org/10.1016/j.compositesa.2006.12.006 [compTest 200].
[11] Falzon PJ, Herszberg I. Mechanical performance of 2-d braided carbon/epoxy composites. Compos Sci Technol 1998;58(2):253–65. http://dx.doi.org/10.1016/S0266-3538(97)00133-4 [Australasian special issue on manufacturing processes and mechanical properties characterisation of advanced composites].
[12] Viju S, Thilagavathi G. Fabrication and characterization of silk braided sutures. Fibers Polym 2012;13(6):782–9. http://dx.doi.org/10.1007/s12221-012-0782-8.
[13] Davies P, Reaud Y, Dussud L, Woerther P. Mechanical behaviour of hmpe and aramid fibre ropes for deep sea handling operations. Ocean Eng 2011;38(17–18):2208–14. http://dx.doi.org/10.1016/j.oceaneng.2011.10.010.
[14] McKenna H, Hearle J, O'Hear N. 4 – properties of rope. In: McKenna H, Hearle J, O'Hear N, editors. Handbook of fibre rope technology. Woodhead publishing series in textiles. Woodhead Publishing; 2004. p. 101–40. http://dx.doi.org/10.1533/9781855739932.101.
[15] Sakaguchi M, Nakai A, Hamada H, Takeda N. The mechanical properties of unidirectional thermoplastic composites manufactured by a micro-braiding technique. Compos Sci Technol 2000;60(5):717–22. http://dx.doi.org/10.1016/S0266-3538(99)00175-X.
[16] Fujihara K, Huang Z-M, Ramakrishna S, Hamada H. Influence of processing conditions on bending property of continuous carbon fiber reinforced peek composites. Compos Sci Technol 2004;64(16):2525–34. http://dx.doi.org/10.1016/j.compscitech.2004.05.014.
[17] ASTM standard D1577-07. Standard test methods for linear density of textile fibers. In: ASTM international, West Conshohocken, PA; 2012. http://dx.doi.org/10.1520/D1577-07R12.
[18] ASTM standard D3171. Standard test methods for constituent content of composite materials. In: ASTM international, West Conshohocken, PA; 2011. http://dx.doi.org/10.1520/D3171-11.

[19] ASTM standard ASTMD2734-09. Standard test methods for void content of reinforced plastics. In: ASTM international, West Conshohocken, PA; 2009. http://dx.doi.org/10.1520/D2734-09.
[20] Berger L, Kausch H, Plummer C. Structure and deformation mechanisms in uhmwpe-fibres. Polymer 2003;44(19):5877–84. http://dx.doi.org/10.1016/S0032-3861(03)00536-6.
[21] Van Der Werff H, Pennings A. Tensile deformation of high strength and high modulus polyethylene fibers. Colloid Polym Sci 1991;269(8):747–63. http://dx.doi.org/10.1007/BF00657441.
[22] Marissen R. Design with ultra strong polyethylene fibers. Mater Sci Appl 2011;2(5):319–30. http://dx.doi.org/10.4236/msa.2011.25042.
[23] McKenna H, Hearle J, O'Hear N, Institute T. Handbook of fibre rope technology. Woodhead publishing in textile technology series. CRC Press; 2004.
[24] Briscoe B, Motamedi F. The ballistic impact characteristics of aramid fabrics: the influence of interface friction. Wear 1992;158(1-2):229–47. http://dx.doi.org/10.1016/0043-1648(92)90041-6.
[25] ASTM standard ASTMD3039-08. Standard test method for tensile properties of polymer matrix composite materials. In: ASTM international, West Conshohocken, PA; 2008.
[26] Russell B, Karthikeyan K, Deshpande V, Fleck N. The high strain rate response of ultra high molecular-weight polyethylene: from fibre to laminate. Int J Impact Eng 2013;60(0):1–9.
[27] Karthikeyan K, Russell B, Fleck N, Wadley H, Deshpande V. The effect of shear strength on the ballistic response of laminated composite plates. Eur J Mech – A/Solids 2013;42(0):35–53.